A General Critique of
Inertial-Electrostatic Confinement
Fusion Systems

by

Todd H. Rider

S.M. and S.B., Electrical Engineering
MIT, 1991

Submitted to the Department of Nuclear Engineering
in partial fulfillment of the requirements for the degree of

Master of Science

at the

MASSACHUSETTS INSTITUTE OF TECHNOLOGY

May 1994

© Todd H. Rider 1994

The author hereby grants to MIT permission to reproduce and
to distribute copies of this thesis document in whole or in part.

Signature of Author_____
Department of Nuclear Engineering
April 15, 1994

Certified by_____
Lawrence M. Lidsky
Professor of Nuclear Engineering
Thesis Supervisor

Certified by_____
Louis D. Smullin
Professor of Electrical Engineering
Thesis Reader

Accepted by_____
Allan F. Henry
Chairman, Department Committee on Graduate Students

A General Critique of

Inertial-Electrostatic Confinement

Fusion Systems

by

Todd H. Rider

Abstract

The suitability of various implementations of inertial-electrostatic confinement (IEC) systems for use as D-T, D-D, D-^{3}He, p-^{11}B, and p-^{6}Li reactors is examined; these IEC designs create a deep electrostatic potential well within the plasma in order to confine and accelerate ions, and they typically use magnetic fields or electrostatic grids to confine electrons. It is shown that while an IEC reactor would have the advantages of high power densities and relatively simple engineering design when compared with other fusion schemes, it suffers from several flaws. Foremost among these problems is that on the basis of velocity-space diffusion calculations, it does not appear to be possible for the dense central region of a reactor-grade device to maintain significantly non-Maxwellian ion distributions or to keep two different ion species at significantly different temperatures; this discovery contradicts earlier claims of the particular suitability of IEC systems for advanced fuels. Since the ions form a Maxwellian distribution with a mean energy not very much smaller than the electrostatic well depth, ions in the energetic tail of the distribution will likely be lost at rates greatly in excess of the fusion rate. Furthermore, even optimistic assumptions about the performance of the surrounding polyhedral cusp magnetic field lead to the conclusion that the electron losses from the machine will be intolerable for all fuels except DT. If electrostatic grids are used instead of magnetic cusps, the particle losses should be even worse. Finally, because the Maxwellian ion distributions are not fundamentally different than those in other fusion schemes, bremsstrahlung losses will be similar; in particular, the ratio of bremsstrahlung power to fusion power will at best be $\sim$1.7 for p-^{11}B and $\sim$5.4 for p-^{6}Li, demonstrating that IEC cannot utilize proton-based fuels in a practical manner. In order for IEC systems to be used as fusion reactors, it will be necessary to find methods to circumvent these problems.

Thesis Supervisor: Lawrence M. Lidsky
Title: Professor of Nuclear Engineering

Acknowledgements

Contents

List of Figures

Chapter 1

Introduction

Inertial-electrostatic confinement (IEC) involves the creation of deep electrostatic potential wells within a plasma in order to accelerate ions up to energies sufficient for fusion reactions to occur. These potential wells can be created and maintained by a slight excess of electrons in a certain region of the plasma or by electrostatic grids. Typically such systems are arranged in a spherical geometry, as illustrated in Figure 1-1, taken from [1]. Some of the earliest work on such systems was performed by Elmore, Tuck, and Watson [2], Farnsworth [3, 4], and Hirsch [5, 6]. A slightly different implemention has been described by Barnes, Nebel, and Turner[7].

Recently the fundamental IEC concept has been modified by Bussard [1, 8] to include a surrounding polyhedral cusp magnetic field in order to improve electron confinement; this type of system has been analyzed by Krall and Rosenberg [9, 10] and is depicted in Figure 1-2 (from ref. [1]).

Another recent suggestion by Bussard [11], as well as Barnes and Turner [12], is to use driven acoustic standing waves to increase the average density in the core of the device. Such a process is illustrated in Figure 1-3 as originally presented in [11]. Following the convention of Bussard, this technique will be referred to as the inertial-collisional
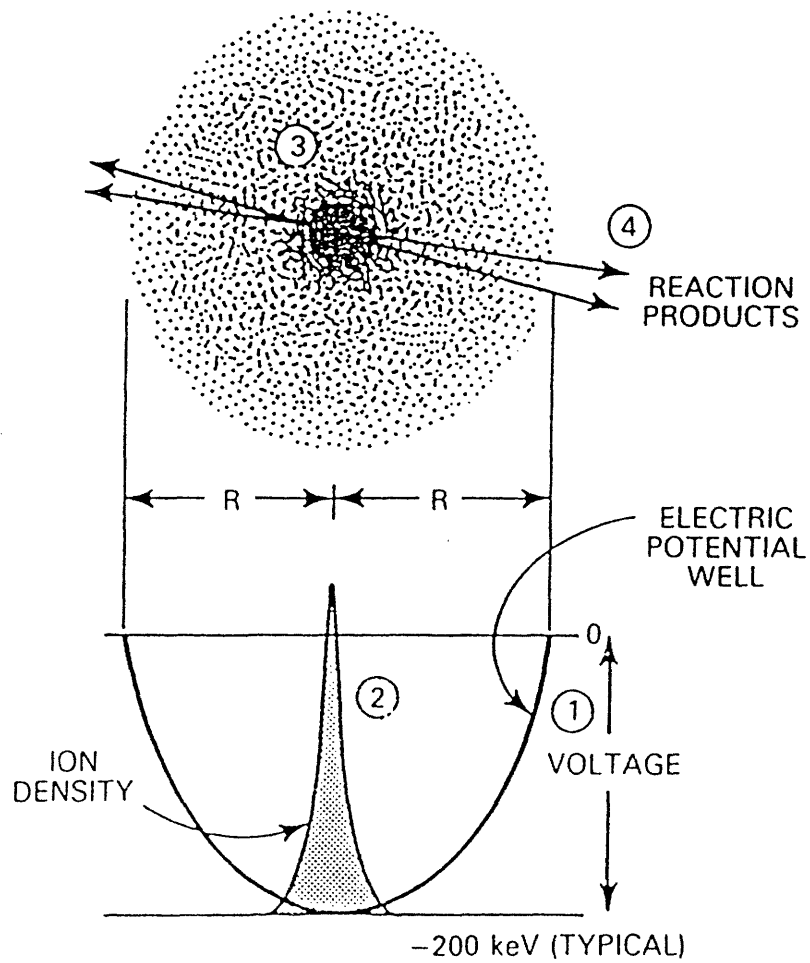
Inertial-electrostatic confinement: deep negative electric potential well ① traps positive ion fuels ② in spherical radial oscillations ③ until they make fusion reactions ④.

Figure 1-1: Inertial-Electrostatic Confinement

8

ION
SOURCE

ELECTRON
GUN
INJECTED
ELECTRONS

MAGNET
FIELD
COILS

MAGNETIC
FIELD LINES
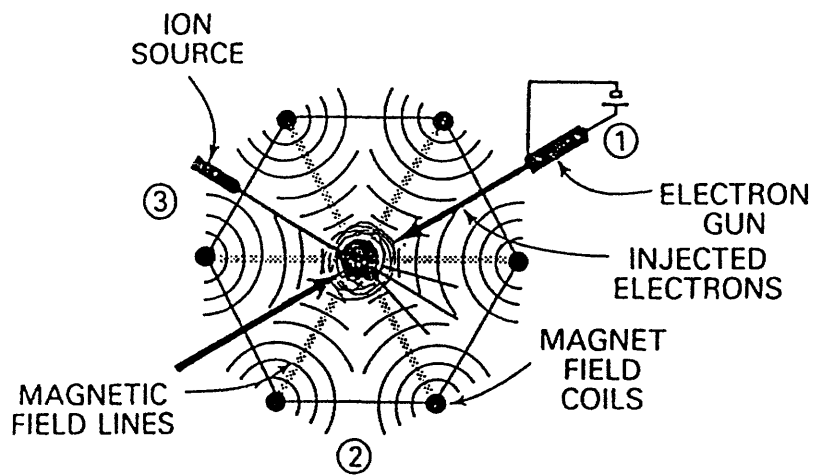
Inertial-electrostatic confinement: trapping well
formed by energetic electron injection ① into cusps
of polyhedral magnetic fields ② and ions fall into
well and remain until reacted ③.

Figure 1-2: Addition of Polyhedral Cusp Magnetic Field

9

compression effect, or the ICC effect.

It has been suggested [1, 10] that IEC can maintain non-Maxwellian ion distributions at fusion reactor parameters; it has been further suggested in [1] that the two ion species may be kept at significantly different energies. Both of these properties would confer the ability for the fusion device to exploit resonance peaks in fusion cross sections more fully than other systems can. Such a machine would then be highly suitable for use with advanced fuels like D-^{3}He and p-^{11}B. Reactions using these fuels have the advantage of producing virtually all of their power in the form of charged particles which can be directly converted to electricity at very high efficiencies, as depicted in Figure 1-4 (from [1]). Since few neutrons are produced by burning these advanced fuels, radiation shielding requirements and the activation of structural materials become much less worrisome problems.

In addition to being able to use advanced fuels efficiently, IEC-based reactors might be able to offer higher power densities and simpler engineering designs than other fusion approaches. If these many advantages could be realized, IEC would overcome the objections that have been raised concerning more conventional fusion schemes [13].

The object of this paper is to examine various critical physics issues in as general a fashion as possible, so that the results will apply to a wide range of IEC systems and related variants. In particular, the potential problems which are analyzed include ion thermalization, ion losses, electron losses, bremsstrahlung emission, and synchrotron radiation losses.

The following conventions are adopted throughout the paper, except where it is explicitly stated otherwise. Temperatures and energies are in eV and all other quantities are in cgs units. If a species j is monoenergetic then $T_j \equiv \frac{2}{3}E_j$.

10
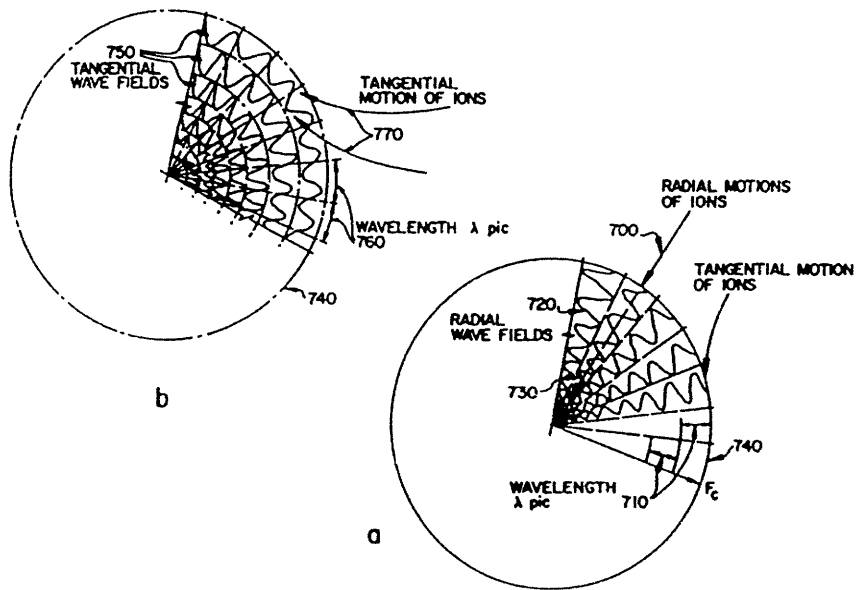
Figure 1-3: Acoustic Wave Compression of IEC Plasma Core

COLLECTOR SHELL
AT HIGH POSITIVE
VOLTAGE ②

INSULATORS

+1 MeV (TYPICAL)

EXTERNAL
ELECTRIC
FIELD

VOLTAGE

0

INTERNAL ION
TRAPPING WELL

−200 keV (TYPICAL)
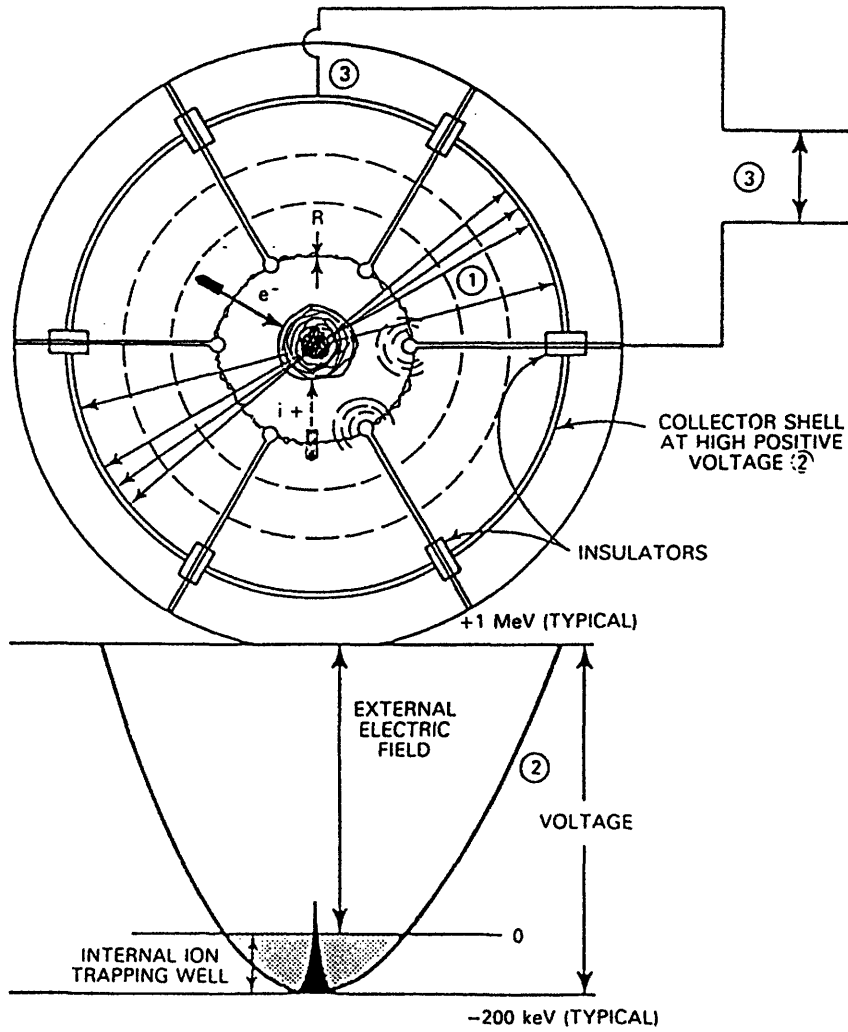
Direct electric conversion: reaction products ① are energetic charged particles, which escape against spherically symmetric radial voltage gradient ② to yield radiation-free direct electric power output ③.

Figure 1-4: Direct Electric Conversion

12

Chapter 2

General Physics Issues

All of the issues examined in this section are effects that are essentially independent of the densities and density profiles which are used in the inertial-electrostatic fusion device (except for the very weak dependence on density contained in the Coulomb logarithm).

In performing these generalized calculations, the following assumptions have been made:

- There is no spatial variation of temperature or energy in the region of the device where the density is appreciable. (The potential well is assumed to have a broad, flat central region [1, 9].)

- Other regions have low enough densities that most collision-related effects (eg. fusion, bremsstrahlung, and ion-electron heating) are negligible there.

- Velocity distributions in the region of significant density are approximately isotropic.

- The spherical geometry returns scattered ions to the dense center of the device, so that only the parallel component of velocity-space diffusion must be considered. (In reality there will be some buildup of angular momentum due to perpendicular

velocity space diffusion in regions other than the exact center; this problem is treated in [10].)

- There is no spatial variation in fuel stoichiometry (n_{i1}/n_{i2}, the ratio of the densities of the two ion species i1 and i2) in the region of appreciable density.

- Quasineutrality ($n_e = Z_{i1}n_{i1} + Z_{i2}n_{i2}$, in which n_e is the electron density, while Z_{i1} and Z_{i2} are the charges of the two ion species) holds in the region of significant density.

2.1 Fusion Power Density

The gross power per volume produced by the fusion of two different ion species i1 and i2 is

$$\frac{P_{fus}}{V} = 1.602 \cdot 10^{-19} < \sigma v > Q n_{i1} n_{i2} \; \frac{\text{Watts}}{\text{cm}^3} \; , \qquad (2.1)$$

where σ is the fusion cross section, v is the characteristic velocity, Q is the energy (in eV) released per reaction, and n_{i1} and n_{i2} are the densities of the two ion species. All quantities other than energy are in cgs units. In the case of fusion of a single ion species (eg. D-D reactions), $n_{i1} n_{i2}$ in the above formula is replaced by $\frac{1}{2}n_i^2$ to avoid counting the same reactions twice.

The fusion power can be expressed in terms of the ratio of the ion densities, $x \equiv n_{i1}/n_{i2}$. If the first ion species has a charge of one and the second ion species has charge Z_2, quasineutrality stipulates that $n_e = n_{i1} + Z_2 n_{i2}$. Using these facts the fusion power density becomes

$$\frac{P_{fus}}{V} = 1.602 \cdot 10^{-19} < \sigma v > Q \frac{x}{(x + Z_2)^2} n_e^2 \; \frac{\text{Watts}}{\text{cm}^3} \; . \qquad (2.2)$$

Note that the fusion power is maximized for $x = Z_2$. Contrary to what one may initially think, the power is not maximum for $x = 1$ since it is the total charge, not total

14

number of ions, which is being held constant as the fuel mixture is changed. The total charge is limited in general by the structure and strength of the confining electric and magnetic fields.

For the purpose of comparisons with other characteristic times in the device, the characteristic fusion time of a test i1 ion with a member of the i2 ion species is readily defined (here $n_{i\,eff}$ is the effective ion density seen by the test ion as it transits the system):

$$\tau_{fus} = \frac{1}{n_{i2\,eff} < \sigma v >} \, .$$ (2.3)

2.2 Energy Equilibration Between Ion Species

It is worthwhile to check whether one ion species can be maintained at a significantly lower energy than the other ion species. To do so, it will be assumed that the i1 species is more energetic than the i2 species and that (at least to a first approximation) the standard Spitzer-type expression for interspecies energy transfer may be applied to this problem.

As discussed in Glasstone and Lovberg [14] and Book [15], the heating of the i2 species by the i1 ions may be described by

$$\frac{dT_{i2}}{dt} = \frac{8}{3}\sqrt{2\pi} \, e^4 \frac{\sqrt{m_{i1}m_{i2}} Z_{i1}^2 Z_{i2}^2 n_{i1} \ln \Lambda_{i1-i2}}{(m_{i1}T_{i2} + m_{i2}T_{i1})^{3/2}} (T_{i1} - T_{i2}) \, ,$$ (2.4)

in which all quantities are in cgs units.

Converting all temperatures and energies to eV and evaluating the constants, one obtains:

$$\frac{dT_{i2}}{dt} = 1.75 \cdot 10^{-19} \frac{\sqrt{m_{i1}m_{i2}} Z_{i1}^2 Z_{i2}^2 n_{i1} \ln \Lambda_{i1-i2}}{(m_{i1}T_{i2} + m_{i2}T_{i1})^{3/2}} (T_{i1} - T_{i2}) \, .$$ (2.5)

15

Because of the presumed Maxwellian distribution of i2 ions, the power density transferred to them by the i1 ions is

$$\frac{P_{i1-i2}}{V} = \frac{3}{2}n_{i2}1.75 \cdot 10^{-19}\frac{\sqrt{m_{i1}m_{i2}}Z_{i1}^2 Z_{i2}^2 n_{i1}\ln\Lambda_{i1-i2}}{(m_{i1}T_{i2} + m_{i2}T_{i1})^{3/2}}(T_{i1} - T_{i2})\,. \qquad (2.6)$$

It is now possible to consider two distinct cases. In the first case, T_{i2} is determined by balancing this heat transfer rate from i1 ions with the cooling effect due to the replacement of fused i2 ions with cold i2 ions. The second case is the situation in which the i2 ions are somehow actively refrigerated to insure that they remain at very low energies.

Proceeding with the evaluation of the first case, the cooling rate of i2 ions due to the replacement of fused ions is:

$$\frac{P_{cool}}{V} = \frac{3}{2}T_{i2}n_{i1}n_{i2} < \sigma v >\,. \qquad (2.7)$$

The equilibrium temperature of the i2 species is determined by setting the total amounts of heating and cooling equal to each other. Since both the heating and cooling expressions have the same dependence on the ion densities, integrating them over the region of interest has no effect on the ratio between them. Solving for the equilibrium temperature and defining the ion mass as a multiple of the proton mass m_p, $m_i \equiv \mu_i m_p$, produces the result:

$$T_{i2} = T_{i1}\left[1 + \frac{7.40 \cdot 10^6 < \sigma v > (\mu_{i1}T_{i2} + \mu_{i2}T_{i1})^{3/2}}{\sqrt{\mu_{i1}\mu_{i2}}Z_1^2 Z_2^2 \ln\Lambda_{i1-i2}}\right]^{-1}\,. \qquad (2.8)$$

For the fuels of interest (D-T, D-^{3}He, p-^{11}B, etc.) typical values of the parameters are $< \sigma v > \sim 10^{-16} - 10^{-15}$ cm^3/sec, $T_{i1} \sim 5 \cdot 10^4 - 6 \cdot 10^5$ eV, and $\ln\Lambda_{i1-i2} \sim 15 - 20$. By inserting any values within this range of parameters into the above formula, it is clear that

16

$$.95T_{i1} \leq T_{i2} \leq T_{i1} \; . \tag{2.9}$$

Therefore from the evaluation of this first case it does not appear possible to keep one ion species at a significantly lower temperature or energy than the other without providing additional means of cooling the i2 species.

Moving on to the second case in which a large temperature difference between the ion species is maintained by somehow actively refrigerating one species, it can be shown that the energy transfer rate required to sustain the nonequilibrium state would be prohibitively large. For this purpose assume that $T_{i1} \gg T_{i2}$, so that the collisions between the two ion species occur at a velocity $v \approx \sqrt{3T_{i1}/m_{i1}}$. Coulomb collisions will then transfer energy between the species at the rate calculated above. Dividing this energy transfer rate by the fusion power, one obtains:

$$\frac{P_{i1-i2}}{P_{fus}} = 1.20 \cdot 10^{-13} \left(\frac{m_{i1}}{m_{i2}}\right) \frac{Z_{i1}^2 Z_{i2}^2 \ln \Lambda_{i1-i2}}{\sigma Q T_{i1}} \; . \tag{2.10}$$

For a numerical estimate it is illustrative to use the case of p-^{11}B reactions, for which it would be desirable to have high-energy protons (i1 species) and low-energy boron ions (i2 species). The peak of the fusion cross section, $\sigma \approx 8 \cdot 10^{-25}$ cm^2, occurs for a proton energy of about 620 keV, or $T_{i1} = \frac{2}{3}(620{,}000 \text{ eV})$. Estimating the Coulomb logarithm as approximately 15, the power ratio is found to be:

$$\frac{P_{i1-i2}}{P_{fus}} \approx 1.4 \; . \tag{2.11}$$

If it were possible to operate the reactor with boron ions maintained at very low energies, the boron ions would siphon off more power from the energetic protons than would be produced from the nuclear reactions. In order to keep the system operating precisely at the resonance peak of the reaction cross section, it would then be necessary

to renew the protons' energy and refrigerate the boron ions; otherwise, the temperatures of the two species would rapidly equilibrate as in the first case. The task of continually adding so much energy to one species, subtracting it from the other, and extracting the resulting entropy from the system appears daunting at best.

Thus both from the derivation of the natural energy equilibrium between ion species and from the calculated energy transfer required to keep the system in the nonequilibrium energy state, it does not appear to be possible to maintain one ion species at a significantly higher energy than the other.

Even if both species can still be kept monoenergetic (but at approximately the same energy), the fact that $< \sigma v >$ must be averaged over all collision angles then implies that it is impossible to exploit the resonance peaks of fusion cross sections (eg. the sharp peaks in the p-^{11}B cross section) as fully as might be hoped.

2.3   Ion Thermalization

The ions will begin to evolve from their assumed initial monoenergetic distribution toward a Maxwellian distribution on a timescale characterized by the ion-ion collision time [16]:

$$\tau_{i1-i1} = \frac{3\sqrt{3}\sqrt{m_{i1}}\; T_{i1}^{3/2}}{8\pi Z_{i1}^4 e^4 n_{i1\;eff} \ln \Lambda_{i1-i1}} = 1.4 \cdot 10^7 \frac{\sqrt{\mu_{i1}}\; T_{i1}^{3/2}}{Z_{i1}^4 n_{i1\;eff} \ln \Lambda_{i1-i1}} . \tag{2.12}$$

The collision time may be compared with the fusion time, such that

$$\frac{\tau_{i1-i1}}{\tau_{fus}} = 1.4 \cdot 10^7 \frac{\sqrt{\mu_{i1}}\; T_{i1}^{3/2}}{Z_{i1}^4 \ln \Lambda_{i1-i1}} < \sigma v > \frac{n_{i2}}{n_{i1}} . \tag{2.13}$$

Once again using the typical values of $< \sigma v > \sim 10^{-16} - 10^{-15}$ cm^3/sec, $T_{i1} \sim 5 \cdot 10^4 - 6 \cdot 10^5$ eV, and $\ln \Lambda_{i1-i1} \sim 15 - 20$, one finds that

$$\frac{\tau_{i1-i1}}{\tau_{fus}} \sim 10^{-3} - 10^{-2} \, . \tag{2.14}$$

Thus in the vicinity of the initial ion velocity, the ion distribution will begin to assume a Maxwellian form on a timescale which is two to three orders of magnitude faster than the fusion time. Of course the high-energy tail will require several collision times to fill in, but even so it is apparent that the ion distributions will be essentially Maxwellian. It is also worth noting that the distribution will be truncated at the well depth energy, since the energetic tail can escape from the confining potential well.

Because the ion distributions are Maxwellian to a good approximation, all of the fusion cross sections must be Maxwellian-averaged. One must therefore make do with the same $< \sigma v >$ values as are used in other fusion devices, and resonance peaks in the cross sections cannot be utilized more efficiently than in other types of reactors. In fact, because the high-energy tail of the Maxwellian is truncated at the well depth, the average fusion reactivities will actually be somewhat lower than truly Maxwellian-averaged quantities.

2.4 Ion Upscattering Losses

The ion losses due to radial energy upscattering can now be calculated. Ions can be lost either by completely escaping from the system or by climbing high enough in the well that the strong magnetic field near the plasma boundary deflects them into useless orbits. Both of these effects require that the ions be upscattered by a certain increment in energy.

Consider the upscattering of a test i1 ion with charge Z_{i1} by field ions of both species. (The derivation that follows is an expanded version of an original derivation by M. Rosenberg and N.A. Krall [17].)

Sivukhin [18] gives suitable velocity-space diffusion coefficients for test ions (denoted by subscript t) amid a background of field ions which have an isotropic velocity distribution. The diffusion coefficients for monoenergetic background ions and Maxwellian

19

background ions are the same to within a factor of two; to emphasize the upscattering losses that can occur even if one assumes an initially monoenergetic distribution of ions, the coefficient appropriate to monoenergetic ions will be used here:

$$
\begin{aligned}
D_{\parallel} &= \frac{4\pi Z_{i1}^2 e^4 \ln \Lambda_{ii}}{3m_{i1}^2 v_{i1\,t}^3} \sum_i Z_i^2 n_{i\,eff} v_i^2 \\
&= \frac{4\pi Z_{i1}^4 e^4 n_{i1\,eff} \ln \Lambda_{ii} v_{i1}^2}{3m_{i1}^2 v_{i1\,t}^3} \left[1 + \left(\frac{Z_{i2}}{Z_{i1}}\right)^2 \left(\frac{n_{i2}}{n_{i1}}\right) \left(\frac{m_{i1}}{m_{i2}}\right) \right] ,
\end{aligned} \qquad (2.15)
$$

in which it has been assumed that the two ion species have the same temperature.

The diffusion coefficient may be related to Miyamoto's collision time for i1-i1 collisions:

$$
D_{\parallel} = \frac{1}{6} v_{i1}^2 \left(\frac{v_{i1}}{v_{i1\,t}}\right)^3 \left[1 + \left(\frac{Z_{i2}}{Z_{i1}}\right)^2 \left(\frac{n_{i2}}{n_{i1}}\right) \left(\frac{m_{i1}}{m_{i2}}\right) \right] \frac{1}{\tau_{i1-i1}} . \qquad (2.16)
$$

Using the velocity-space diffusion equation and recognizing that the test ion's velocity can be related to the field ion velocity which it originally had by $v_{i1\,t} = v_{i1}(1 + \Delta v_{i1\,t}/v_{i1})$, one can calculate the time required for ions to be upscattered to velocities high enough for loss from the system:

$$
\tau_{loss} \approx \frac{v_{i1}^2}{D_{\parallel}} \left(\frac{\Delta v_{i1\,t}}{v_{i1}}\right)^2 = 6 \left(\frac{\Delta v_{i1\,t}}{v_{i1}}\right)^2 \left(1 + \frac{\Delta v_{i1\,t}}{v_{i1}}\right)^3 \left[1 + \left(\frac{Z_{i2}}{Z_{i1}}\right)^2 \frac{n_{i2}}{n_{i1}} \frac{m_{i1}}{m_{i2}} \right]^{-1} \tau_{i1-i1} .
$$
$$ (2.17) $$

The loss time can be rewritten in terms of the energy upscattering, $\Delta E/E = 2\Delta v/v$, so that

$$
\tau_{loss} = \frac{3}{2} \left(\frac{\Delta E_t}{E_o}\right)^2 \left(1 + \frac{1}{2}\frac{\Delta E_t}{E_o}\right)^3 \left[1 + \left(\frac{Z_{i2}}{Z_{i1}}\right)^2 \left(\frac{n_{i2}}{n_{i1}}\right) \left(\frac{m_{i1}}{m_{i2}}\right) \right]^{-1} \tau_{i1-i1} . \qquad (2.18)
$$

This loss time may be checked by comparing it with the results of an earlier estimate of how quickly the tail of the Maxwellian is filled in from an initially monoenergetic distribution, as performed by MacDonald, Rosenbluth, and Chuck [19]:

$$\tau_{tail} = \frac{m_{i1}^2 v_{i1}^3 t}{12\pi Z_{i1}^4 e^4 n_{i1\ eff} \ln \Lambda_{ii}} = \frac{2}{3}\left(1 + \frac{1}{2}\frac{\Delta E_t}{E_o}\right)^3 \tau_{i1-i1} \ . \tag{2.19}$$

In the case that $\Delta E/E$ is of order unity (the typical value expected in IEC devices) and there is no i2 species, these two different expressions for the loss time are seen to be comparable.

The fraction of ions that fuse is just the ratio of the loss and fusion times:

$$\frac{\tau_{loss}}{\tau_{fus}} = 2.1 \cdot 10^7 \left(\frac{\Delta E_t}{E_o}\right)^2 \left(1 + \frac{1}{2}\frac{\Delta E_t}{E_o}\right)^3 \left[1 + \left(\frac{Z_{i2}}{Z_{i1}}\right)^2 \frac{n_{i2}}{n_{i1}}\frac{m_{i1}}{m_{i2}}\right]^{-1} \frac{\sqrt{\mu_{i1}}\ T_{i1}^{3/2} <\sigma v> n_{i2}}{Z_{i1}^4 \ln \Lambda_{ii}}\frac{n_{i2}}{n_{i1}} \ . \tag{2.20}$$

In calculating the amount of energy upscattering which is necessary for loss from the well, one must account for the fact that the well depth energy appears deeper to ions with $Z_{i1} > 1$. The condition for loss is that $E_o + \Delta E_t = Z_{i1} E_{well}$, or

$$\frac{\Delta E_t}{E_o} = Z_{i1}\frac{E_{well}}{E_o} - 1 \ . \tag{2.21}$$

A more complete calculation should also include cooling of the fast ions due to electron drag. As a rough estimate of the importance of electron drag relative to ion-ion upscattering, one may consider the ratio of the ion-electron collision time to the ion-ion collision time, as defined in [16]. Considering only a single ion species for simplicity, it may be seen that

$$\frac{\tau_{ie}}{\tau_{ii}} \approx 21\sqrt{\mu_i}Z_i\left(\frac{T_e}{T_i}\right)^{3/2} \ . \tag{2.22}$$

For the fuels and temperatures characteristic of the proposed IEC systems, the ion-

electron collision time is typically at least an order of magnitude larger than the ion-ion collision time. Therefore it appears doubtful that electron drag effects will substantially reduce the ion upscattering losses.

Another possible mechanism for reducing the upscattering losses is cooling of the ions by charge exchange with neutrals. Unfortunately, while charge exchange may prevent ions from escaping the system, the neutrals themselves are free to escape, potentially carrying a sizeable amount of energy out of the confinement system. Considerable technical problems may also result from the pumping requirements necessary to collect the large quantities of escaping neutrals or ions and replace them with fresh ions. Of course, the presence of appreciable charge exchange effects would ultimately serve to degrade the monoenergetic ion distributions even more quickly than has already been calculated. Because of all of these reasons, the introduction of neutrals into the problem is not a useful solution.

2.5 Bremsstrahlung Radiation Losses

Maxon [20] gives the nonrelativistic and extreme relativistic limits for electron-ion and electron-electron bremsstrahlung and interpolates between these two limits to obtain approximate radiation rates in the intermediate regime. His results may be used as a guideline for the necessary corrections for mildly relativistic ($T_e \sim 100$ keV) electrons (consult McNally [21] for a commentary on the empirical expression for bremsstrahlung in this regime). Adding together the expressions for ion-electron and electron-electron bremsstrahlung and defining

$$Z_{eff} \equiv \frac{\sum_i Z_i^2 n_i}{n_e} = \frac{x + Z_2^2}{x + Z_2} \tag{2.23}$$

produces the result that the total bremsstrahlung power per volume is:

$$\frac{P_{br}}{V} = \frac{64\sqrt{2\pi}e^6}{3m_e^{3/2}c^3h} n_e^2 \sqrt{T_e} \left\{ Z_{eff} \left[1 + .7936\frac{T_e}{m_ec^2} + 1.874\left(\frac{T_e}{m_ec^2}\right)^2 \right] + \frac{3}{\sqrt{2}}\frac{T_e}{m_ec^2} \right\} \ , \ \text{or}$$

$$(2.24)$$

$$\frac{P_{br}}{V} = 1.69 \cdot 10^{-32} n_e^2 \sqrt{T_e} \left\{ Z_{eff} \left[1 + .7936\frac{T_e}{m_ec^2} + 1.874\left(\frac{T_e}{m_ec^2}\right)^2 \right] + \frac{3}{\sqrt{2}}\frac{T_e}{m_ec^2} \right\} \frac{\text{Watts}}{\text{cm}^3} \ .$$

$$(2.25)$$

Once again using the expression given by Glasstone and Lovberg [14] and Book [15] for energy transfer between plasma species, the heating of electrons by ions may be described by

$$\frac{dT_e}{dt} = 1.75 \cdot 10^{-19} \sum_i \frac{\sqrt{m_e m_i}Z_i^2 n_i \ln \Lambda_{ei}}{(m_iT_e + m_eT_i)^{3/2}}(T_i - T_e) \ . \tag{2.26}$$

Because of the Maxwellian distribution of electrons, the power density transferred to them by the ions is $\frac{3}{2}n_e$ times the heating rate of Equation 2.26. After converting the power to Watts and assuming that $T_e \gg \frac{m_e}{m_i}T_i$, the result is

$$\frac{P_{ie}}{V} = 7.61 \cdot 10^{-28} n_e \sum_i \frac{Z_i^2 n_i \ln \Lambda_{ei}}{\mu_i T_e^{3/2}}(T_i - T_e) \frac{\text{Watts}}{\text{cm}^3} \ , \tag{2.27}$$

in which the ion masses have been expressed in multiples of the proton mass, $m_i = \mu_i m_p$, temperature is still in eV, and density is in particles/cm^3.

As derived by Rosenbluth [23], there is a correction factor to this expression for ion-electron heating; the correction is caused by partial depletion of the electrons with velocities smaller than the ion thermal velocity, with the net result that

$$\left.\frac{P_{ie}}{V}\right|_{actual} = \frac{P_{ie}}{V} \left[1 - \left(\frac{2\pi^2}{3^{5/4}}\frac{Z_i^2 n_i m_e}{n_e m_i}\frac{T_i}{T_e} \right)^{2/3} \right] \ . \tag{2.28}$$

23

Furthermore, Dawson [22] notes that for relativistic electrons the ion-electron heating must be modified by a factor of $(1 + 0.3T_e/m_ec^2)$. After incorporating the corrections of Rosenbluth and Dawson, the heat transfer rate becomes

$$\frac{P_{ie}}{V} = 7.61 \cdot 10^{-28} n_e \left(1 + \frac{0.3T_e}{m_ec^2}\right) \sum_i \frac{Z_i^2 n_i \ln \Lambda_{ei}}{\mu_i T_e^{3/2}} \left[1 - \left(\frac{5}{1836}\frac{Z_i^2}{\mu_i}\frac{n_i}{n_e}\frac{T_i}{T_e}\right)^{2/3}\right](T_i - T_e) \frac{W}{cm^3} \, .$$

$$(2.29)$$

The equilibrium electron temperature is found by equating the power transferred to the electrons by ion-electron heating with the power lost by the electrons due to bremsstrahlung, synchrotron radiation, ion-electron cooling in the edge of the device, loss of electrons from the system, and other effects. The maximum possible bremsstrahlung rate may be obtained by neglecting all loss mechanisms except bremsstrahlung, thus producing the highest possible equilibrium electron temperature. In this approximation $P_{ie} = P_{br}$. (In the next chapter both synchrotron radiation and edge ion-electron heat transfer will be shown to be negligibly small compared with the bremsstrahlung and heating effects considered here, so this approximation should come close to the actual answer.) Since the ion-electron heating and the bremsstahlung cooling both have the same dependence on the densities (with the exception of the Coulomb logarithm, which slowly varies from about 15 to approximately 20 over the range of the system), integrating over the system volume has essentially no effect. As a result, the equilibrium electron temperature (in eV) can be determined from the general equation:

$$4.494 \cdot 10^4 \left(1 + \frac{0.3T_e}{m_ec^2}\right) \sum_i \frac{Z_i^2 n_i \ln \Lambda_{ei}}{\mu_i n_e} \left[1 - \left(\frac{5}{1836}\frac{Z_i^2}{\mu_i}\frac{n_i}{n_e}\frac{T_i}{T_e}\right)^{2/3}\right](T_i - T_e)$$

$$= T_e^2 \left\{ Z_{eff}\left[1 + .7936\frac{T_e}{m_ec^2} + 1.874\left(\frac{T_e}{m_ec^2}\right)^2\right] + \frac{3}{\sqrt{2}}\frac{T_e}{m_ec^2}\right\} \, . \quad (2.30)$$

After finding the equilibrium electron temperature, it may be used to calculate the

24

fraction of the gross fusion power output which is radiated away by bremsstrahlung:

$$\frac{P_{br}}{P_{fus}} = 1.06 \cdot 10^{-13} \frac{\sqrt{T_e}\{Z_{eff}[1 + .7936\frac{T_e}{m_e c^2} + 1.874(\frac{T_e}{m_e c^2})^2] + \frac{3}{\sqrt{2}}\frac{T_e}{m_e c^2}\}}{<\sigma v > Q\frac{x}{(x+Z_2)^2}} . \qquad (2.31)$$

As stated earlier, these values for the electron temperature and bremsstrahlung have been calculated assuming that bremsstrahlung is the dominant mechanism for cooling of the electrons. This assumption is justified because most of the other possible cooling effects (such as electron cusp losses) would introduce even greater power losses while cooling the electrons and reducing the bremsstrahlung power loss. Although cooling of hot electrons by cold ions in the edge would be a beneficial effect which would not cause further power losses, the very low densities in the edge region stipulate that the total electron cooling there will be much less than the total electron heating in the center of the device.

Chapter 3

Design-Dependent Physics Issues

Included in this section are effects that depend on the specific density, density profiles, and confinement system (eg. magnetic cusp, grids, etc.) which are employed. The first section will outline the specific assumptions made about the spatial density and energy profiles of the devices, and subsequent sections will use these profiles to calculate the magnitude of the various effects.

3.1   Spatial Profiles

3.1.1   Devices with Convergence-Limited Core Densities

In the simplest IEC concepts, the core density is determined solely by the convergence of the spherical flow in the potential well. In the following calculations, it will be assumed that the device employs a single potential well. The theoretical analysis may be simplified by dividing the interior of the machine into three regions: the core ($0 < r < r_c$), the mantle ($r_c < r < r_e$), and the edge ($r_e < r < R$). Typically $R \approx 100 r_c$ and $r_e \sim 50 - 80 r_c$. The following approximate forms for the particle densities and energies are assumed.

Both the electron and ion densities are constant in the core, then because of conservation of particles in the nearly flat part of the potential well, they drop off like $1/r^2$ in the mantle, and they finally reach a constant value in the edge:

$$n_{e,i} = \begin{cases} (n_c)_{e,i} & 0 < r < r_c \\ (n_c)_{e,i}(r_c/r)^2 & r_c < r < r_e \\ (n_c)_{e,i}(r_c/r_e)^2 & r_e < r < R \,. \end{cases} \tag{3.1}$$

A graph of the density is given in Figure 3-1, taken from [9].

Electrons in the core and mantle are heated enough by Coulomb friction with the energetic ions that they will tend to form a Maxwellian distribution with a temperature of T_{eo}. As the electrons travel from the center to the edge of the well, they acquire additional energy corresponding to the well depth, so that the electron energy distribution is given by

$$E_e = \begin{cases} \frac{3}{2}T_{eo} & 0 < r < r_e \\ \frac{3}{2}T_{eo} + E_w f(r) & r_e < r < R \,, \end{cases} \tag{3.2}$$

for which $f(r)$ is some rapidly increasing function of r such that $f(r_e) = 0$ and $f(R) = 1$.

Similarly, the ion energies have the following spatial variation:

$$E_i = \begin{cases} \frac{3}{2}T_{io} & 0 < r < r_e \\ \frac{3}{2}T_{io} - E_w Z_i f(r) & r_e < r \,. \end{cases} \tag{3.3}$$

Figure 3-1 (from [9]) presents a graph of the potential well shape.

To a first approximation bremsstrahlung, fusion, and ion-electron heating in the edge may be neglected because of the low densities and ion energies there. Using the fact that $r_e \gg r_c$, the following useful integral over the core and mantle regions is found:

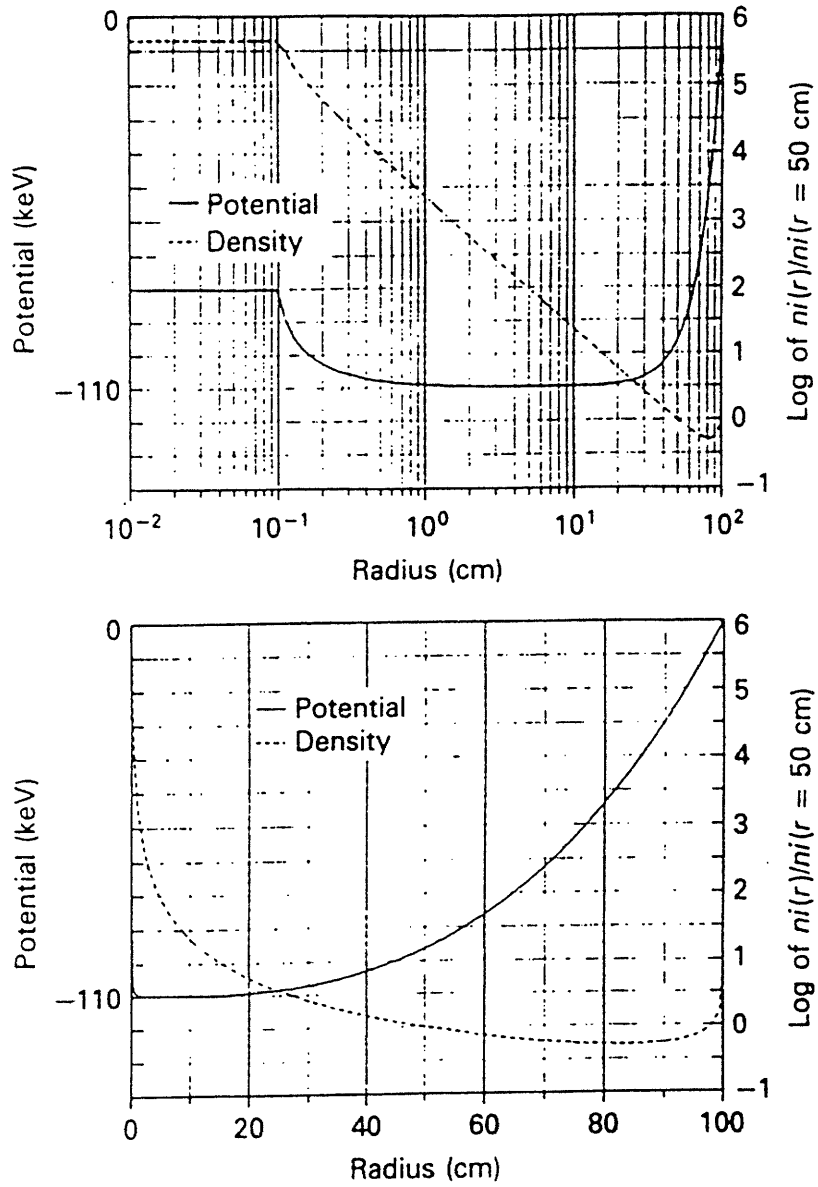$$\int_0^{r_e} n^2 4\pi r^2 dr \approx \frac{16}{3}\pi n_c^2 r_c^3 \,. \tag{3.4}$$

27

Figure 3-1: Density and Potential Well Profiles

3.1.2 Devices with Enhanced Core Densities

Another class of IEC schemes is centered around increasing the core density beyond the convergence-limited value. References [11] and [12] propose to achieve this increase using acoustic standing waves; this phenomenon has been called the inertial-collisional compression (ICC) effect. If the only role of the standing waves is to increase the core density or change the density profile, there will be no significant impact on the problems which have already been analyzed. The primary usefulness of the ICC effect lies being able to affect the total fusion power and hence perhaps the relative severity of electron cusp losses.

If the root mean squared core density of an ICC device is enhanced beyond that of a non-ICC device by a factor of ξ, then the density profile may be approximated as

$$
n_{e,i} = \begin{cases} (n_c)_{e,i} & 0 < r < r_c \\ (n_c)_{e,i}(r_c/r)^2/\xi & r_c < r < r_e \\ (n_c)_{e,i}(r_c/r_e)^2/\xi & r_e < r < R . \end{cases} \tag{3.5}
$$

For simplicity the energy profiles will be considered to remain approximately like those in purely convergence-limited machines.

If the core density is significantly enhanced ($\xi \gg 1$) via the ICC effect or other mechanisms, then essentially only the core will contribute to processes like fusion and bremsstrahlung; the rate of these processes in the mantle will be negligible by comparison. The net result of this fact is that

$$
\int_0^{r_e} n^2 4\pi r^2 dr \approx \frac{4}{3}\pi n_c^2 r_c^3 . \tag{3.6}
$$

29

3.2 Relative Importance of Edge and Central Plasma Regions

One of the key assumptions on which this entire analysis is based is that only the dense central region of the plasma contributes significantly to processes such as bremsstrahlung and ion-electron heat transfer; the edge region is assumed to make a negligible contribution to these processes. This assumption can now be justified.

Effects such as bremsstrahlung and ion-electron heat transfer can be expressed as total powers and are proportional to the density squared times the volume of the region concerned. For a given process, the ratio of the powers of that process in the edge and central (combined core and mantle) regions is

$$\frac{P_{edge}}{P_{core+mantle}} \sim \frac{\int_{r_e}^{R} n^2 4\pi r^2 dr}{\int_{0}^{r_e} n^2 4\pi r^2 dr} \; . \tag{3.7}$$

For a device with convergence-limited core density, Equations 3.1 and 3.4 may be used to express the ratio of integrals from Equation 3.7 as

$$\frac{\int_{r_e}^{R} n^2 4\pi r^2 dr}{\int_{0}^{r_e} n^2 4\pi r^2 dr} = \frac{1}{4} \left(\frac{r_c}{r_e} \right) \left[\left(\frac{R}{r_e} \right)^3 - 1 \right] \; . \tag{3.8}$$

For typical values of $r_e = 50 r_c$ and $R = 2r_e$, the ratio of edge effects to central region effects is

$$\frac{\int_{r_e}^{R} n^2 4\pi r^2 dr}{\int_{0}^{r_e} n^2 4\pi r^2 dr} = 0.035 \; . \tag{3.9}$$

Of course, in computing the ratio of edge effects to central region effects for particular quantities like bremsstrahlung power or power transferred between ions and electrons, the exact answer will involve other numerical factors to account for parameters such as particle temperatures in the edge versus in the core, Coulomb logarithms in the two

30

different regions, etc. Precise evaluation of these factors requires detailed spatial profiles of the electron temperature and ion temperature in the edge region, but in general the net result of the factors will be to change the result above by at most about a factor of two or three. In conclusion, one finds that

$$\frac{P_{edge}}{P_{core+mantle}} \sim 10^{-2} - 10^{-1} \,. \tag{3.10}$$

If the ICC effect is used to enhance the core density relative to the edge density, the ratio of the powers will be even smaller. It is clearly evident that for the purposes of the calculations presented in this paper, the edge region can be neglected in comparison with the central region of the plasma for both non-ICC and ICC designs.

3.3   Total Fusion Power

Using the integral in Equation 3.4 for a machine with convergence-limited core densities, the total fusion power is found to be

$$P_{fus} = 2.68 \cdot 10^{-18} < \sigma v > Q \frac{x}{(x + Z_2)^2} n_{ce}^2 r_c^3 \text{ Watts}, \tag{3.11}$$

where $x \equiv n_{i1}/n_{i2}$, $Z_{i1} = 1$, and $Z_{i2} = Z_2$. The fusion power is maximized for $x = Z_2$.

For a device employing the ICC effect, Equation 3.11 is reduced by a factor of four:

$$P_{fus} = 6.70 \cdot 10^{-19} < \sigma v > Q \frac{x}{(x + Z_2)^2} n_{ce}^2 r_c^3 \text{ Watts}. \tag{3.12}$$

3.4 Electron Cusp Losses

An especially serious power loss mechanism is the loss of energetic electrons through the cusps of the confining magnetic field. At conditions of interest for a fusion reactor, the effective radius r_H of each cusp "hole" through which electrons escape is of the order of the electron gyroradius r_e, so that $r_H = k_H r_e$, where typically $1 \leq k_H < 5$ [24, 25]. The electron gyroradius, in turn, is given by the formula [15]

$$r_e = 2.38 \frac{\sqrt{2E_e}}{B} \text{ cm},$$
(3.13)

in which E_e is in eV and B is in Gauss. Note that a factor of $\sqrt{2}$ has been introduced into the usual formula because at the outer surface of the plasma the electrons are in directed motion [1].

Assuming a spherically symmetric distribution of electrons with essentially radial velocities, the number of electrons that escape each second will be $\frac{1}{2} n_{edge \ e} v_e$ times the total area of the cusp holes. The factor of 1/2 is included because only half of the electrons are traveling outward. If each escaping electron carries away an amount of energy E_{loss} and there are N cusps (thus $N\pi r_H^2$ is the total hole area), then the power loss due to escaping electrons will be

$$P_{e \ loss \ cusp} = \frac{1}{2} N \pi r_H^2 n_{edge \ e} v_e E_{loss}.$$
(3.14)

Noting that $E_{loss} = E_e = E_{well}$, the well depth energy, and that $v_e = \sqrt{2E_e/m_e}$, and then expressing the power in Watts, energy in eV, and everything else in cgs units, one obtains

$$P_{e \ loss \ cusp} = 1.69 \cdot 10^{-10} \frac{N k_H^2 n_{edge \ e} E_{well}^{5/2}}{B^2} \text{ Watts}.$$
(3.15)

If there is no ICC enhancement of the core density, then the fraction of power which is lost because of escaping electrons is

$$\frac{P_{e\ loss\ cusp}}{P_{fus}} = 6.30 \cdot 10^7 N k_H^2 \frac{(x + Z_2)^2}{x} \frac{1}{<\sigma v > Q} \frac{n_{edge\ e} E_{well}^{5/2}}{B^2 n_{ce}^2 r_c^3} . \qquad (3.16)$$

If the ICC effect is used to enhance the core density significantly, the vast majority of the fusion power will only come from the core, so the above expression should be multiplied by four.

Now one makes the assumption that the edge of the plasma has $\beta = 1$ [26, 27], or $B^2 = 8\pi n_{edge\ e} E_{well}$, for E_{well} in ergs. Putting the energy in eV and substituting into Equation 3.16, the ratio of cusp loss power to fusion power can be simplified somewhat:

$$\frac{P_{e\ loss\ cusp}}{P_{fus}} = 1.56 \cdot 10^{18} N k_H^2 \frac{(x + Z_2)^2}{x} \frac{1}{<\sigma v > Q} \frac{E_{well}^{3/2}}{n_{ce}^2 r_c^3} . \qquad (3.17)$$

One might think that using the ICC effect to increase the core density relative to the edge density would improve the ratio of cusp losses to fusion power, since the cusp losses occur at the edge and fusion occurs in or near the core. Yet as indicated in Equation 3.17, the constraint that $\beta = 1$ at the outer plasma boundary removed the dependence of the power loss fraction on the edge density, and thus on the density profile. It appears that using acoustic waves to alter the density profile of the device will create no significant improvement in reactor performance, provided that the waves only act to alter the density profile. The only critical parameter is the core density, which may be created via the ICC effect or simply by unaided ion flow convergence at the center of the device.

The electron power loss fraction is minimized for $x = Z_2$, at which

$$\frac{P_{e\ loss\ cusp}}{P_{fus}} = 6.26 \cdot 10^{18} N k_H^2 Z_2 \frac{E_{well}^{3/2}}{<\sigma v > Q n_{ce}^2 r_c^3} . \qquad (3.18)$$

An expression for the characteristic electron loss time can also be derived. One begins

by noting that the fraction of electrons lost during each pass through the system will just be the total area of the cusp holes divided by the surface area of the machine. If this loss fraction is made small enough to be practical, then G_e, the average number of transits an electron makes through the system before being lost, is well approximated as just the inverse of the loss fraction. Specifically, for N cusps:

$$G_e = \frac{4\pi R^2}{N\pi r_H^2} = .353 \frac{R^2 B^2}{N k_H^2 E_e} \ .$$ (3.19)

The loss time may be expressed as $\tau_{loss} = G_e \tau_{tr}$, where τ_{tr} is the time required for a single transit through the system. This transit time is in turn $\tau_{tr} = 2R/v_{av}$, where v_{av} is the average electron velocity, or

$$v_{av} = A\sqrt{\frac{T_{eo}}{m_e}} \ ,$$ (3.20)

with A some number of order unity to account for the faster electron speed near the edge of the well.

Putting the above equations together, one obtains

$$\tau_{e \ loss \ cusp} = 1.68 \cdot 10^{-8} \frac{R^3 B^2}{N k_H^2 A E_{well} \sqrt{T_{eo}}} \sec \ ,$$ (3.21)

where the temperature and energy are in eV and everything else is in cgs units.

One might be tempted to use electrostatic fields at the cusps in order to reduce the number of escaping electrons or the amount of energy which they carry away. Unfortunately, such techniques would also increase the ion losses or the energy carried away by each escaping ion, and so they are of little interest.

A better method to reduce the electron power losses is to direct-convert the energy of escaping electrons into electricity. In particular, the addition of a "sideways" magnetic field outside each cusp would result in $v \times B$ forces which could separate outgoing escaping electrons from incoming fresh electrons. Then the outgoing electrons could be efficiently

directed around the electron guns, so that they will hit direct-converter grids and return most of their energy to the system.

3.5 Electron Grid Losses

Now consider the power losses that are caused by confining the particles with an electrostatic grid instead of a cusp. The ion losses on the grid can be minimized by making the grid bias large and positive, so that ions hitting the grid will possess essentially zero energy; one must then calculate only the electron grid losses. Assuming that the grid has radius r_{grid} and transparency to electrons η_e, and choosing the electron energy, velocity, and density to be evaluated at the grid, then one obtains:

$$P_{e\ loss\ grid} = (1 - \eta_e)4\pi r_{grid}^2 n_{grid\ e}v_{e\ grid}E_{e\ grid} . \tag{3.22}$$

Noting that $v_e = \sqrt{2E_e/m_e}$ and expressing the power in Watts, energy in eV, and everything else in cgs units, one finds that

$$P_{e\ loss\ grid} = 1.19 \cdot 10^{-10}(1 - \eta_e)r_{grid}^2 n_{e\ grid}E_{e\ grid}^{3/2} \text{ Watts} . \tag{3.23}$$

It is instructive to compare this expression for the grid losses with the earlier expression for total fusion power:

$$\frac{P_{e\ loss\ grid}}{P_{fus}} = 4.45 \cdot 10^7 \frac{(x + Z_2)^2}{x}(1 - \eta_e)\left(\frac{r_{grid}}{r_c}\right)^2 \left(\frac{n_{e\ grid}}{n_{ce}}\right)\frac{E_{e\ grid}^{3/2}}{<\sigma v > Qn_{ce}r_c} . \tag{3.24}$$

Taking $r_{grid} = R$, $n_{e\ grid} = n_{e\ edge} = n_{ce}(r_c/r_e)^2$, $E_{e\ grid} = E_{well}$, and $x = Z_2$, this expression becomes

$$\frac{P_{e\ loss\ grid}}{P_{fus}} = 1.78 \cdot 10^8 Z_2(1 - \eta_e) \left(\frac{R}{r_e}\right)^2 \frac{E_{well}^{3/2}}{<\sigma v> Q n_{ce} r_c} \ . \tag{3.25}$$

This ratio indicates that at typical reactor parameters the grid losses are several orders of magnitude greater than the fusion power. As an illustration of the optimum performance that can be expected, choosing $Z_2 = 1$, $\eta_e = .99$, $R/r_e = 2$, $E_{well} = 60,000$ eV, $<\sigma v> = 10^{-15}$ cm^3/sec, $Q = 2 \cdot 10^7$ eV, $n_{ce} = 10^{18}$ cm^{-3}, and $r_c = 2$ cm, one discovers that

$$\frac{P_{e\ loss\ grid}}{P_{fus}} \sim 3000 \ . \tag{3.26}$$

Not only are the electron losses tremendously greater than the fusion power, but one also has the inherent problem of cooling the grids.

Although one might contemplate passing a current through the grid wires to create a magnetic field around them and reduce the number of particles striking the grid, this idea does not appear to be advisable. Magnetic fields strong enough to deflect particles from the grid wires would also interfere with the desired purely radial motion of the particles, thereby significantly reducing the degree of core convergence in the IEC system.

3.6   Ion Grid Losses

One could attempt to reduce the power losses by putting a large negative bias on the grids; then it will be the ions and not the electrons which constitute most of the power loss upon impact with the grids. By analogy with the electron calculation, it is straightforward to derive the ion losses caused by an electrostatic grid in the system. If the grid ion transparency is η_i then

$$P_{i\ loss\ grid} = (1 - \eta_i) 4\pi r_{grid}^2 n_{i\ grid} v_{i\ grid} E_{i\ grid} \ . \tag{3.27}$$

Noting that $v_i = \sqrt{2E_i/m_i}$ and expressing the power in Watts, energy in eV, and everything else in cgs units, one finds that

$$P_{i \; loss \; grid} = 2.79 \cdot 10^{-12}(1 - \eta_i)r_{grid}^2 n_{i \; grid}E_{i \; grid}^{3/2}/\sqrt{\mu_i} \; \text{Watts} \,. \qquad (3.28)$$

For $\mu_i = 2$ and all other parameters as before, the ion losses will be about 60 times smaller than the corresponding electron losses calculated above; the reason is simply that the ions are moving much more slowly than electrons of the same energy. Unfortunately, the grid losses are still much greater than the fusion power:

$$\frac{P_{i \; loss \; grid}}{P_{fus}} \sim 40 \,. \qquad (3.29)$$

Because of the overwhelming power losses and cooling problems associated with grids, it appears preferable to use a different confinement technique such as the magnetic cusp system.

3.7   Electron Thermalization

Equation 3.21, the electron loss time for a cusp device with convergence-limited core density may be compared with the electron-electron collision time from [16]:

$$\tau_{ee} = \frac{25.8\sqrt{m_e} \; T_e^{3/2}}{16\pi^{3/2}e^4 n_{e \; eff} \ln \Lambda_{ee}} = 3.2 \cdot 10^5 \frac{T_e^{3/2}}{n_{e \; eff} \ln \Lambda_{ee}} \,, \qquad (3.30)$$

where $n_{e \; eff}$ is the root mean square density experienced by an electron circulating through the plasma. If the density profile may be approximated by Equation 3.1 with $R \approx 100 r_c$, n_{eff} will be about an order of magnitude smaller than the core density.

It can be determined whether the electrons will be significantly thermalized by considering the ratio of the two times,

$$\frac{\tau_{ee}}{\tau_{e\,loss\,cusp}} = 1.9 \cdot 10^{13} \frac{T_{eo}^2 N k_H^2 A E_{well}}{\ln \Lambda_{ee} n_{e\,eff} R^3 B^2} \,.$$

(3.31)

For the typical parameters $N = 8$, $k_H = 2$, $A \sim 1.5$, $T_{eo} \sim 2 \cdot 10^4 - 1.5 \cdot 10^5$ eV, $E_{well} \sim 6 \cdot 10^4 - 9 \cdot 10^5$ eV, $\ln \Lambda_{ee} \sim 15 - 20$, $n_{e\,eff} \sim 10^{16} - 10^{17}$ cm^{-3}, $R = 150 - 300$ cm, and $B \sim 10^4 - 10^5$ Gauss, the ratio is found to be in the range

$$\frac{\tau_{ee}}{\tau_{e\,loss\,cusp}} \sim 10^{-6} - 10^{-3} \,.$$

(3.32)

Thus it is readily apparent that electrons in the center of the IEC device will form an essentially Maxwellian distribution.

3.8 Synchrotron Radiation Losses

In calculating the electron temperature and bremsstrahlung losses in the previous chapter, the effects of synchrotron radiation were assumed to be negligibly small. This assumption will now be justified.

The power density of emitted synchrotron radiation is given in [16] as:

$$\frac{P_{syn}}{V} = \frac{4e^4 B^2 n_e}{3m_e^2 c^3} \left(\frac{T_e}{m_e c^2} \right) \left[1 + \frac{5}{2} \left(\frac{T_e}{m_e c^2} \right) \right] \,.$$

(3.33)

Evaluating the constants, defining V_{syn} to be the plasma volume which is under the influence of the magnetic field and emitting synchrotron radiation, and letting f represent the fraction of the radiation which is actually lost (not reflected back into the plasma and reabsorbed there), the synchrotron power becomes

$$P_{syn} = 6.21 \cdot 10^{-28} B^2 n_e T_e \left[1 + \frac{5}{2} \left(\frac{T_e}{m_e c^2} \right) \right] f V_{syn} \text{ Watts.}$$

(3.34)

In a diamagnetic IEC plasma, synchrotron radiation will only come from the outer layer of the plasma. Electron diamagnetism prevents the external magnetic field from penetrating more than a few electron gyroradii into the plasma [26]. Using the fact that in this outer layer $B^2/8\pi = n_e T_e$ and defining the layer's thickness to be $k_H r_e$, the synchrotron power is found to be

$$P_{syn} = 2.50 \cdot 10^{-38} f T_{e\,edge}^2 \left[1 + \frac{5}{2}\left(\frac{T_{e\,edge}}{m_e c^2}\right)\right] n_{edge\,e}^2 \, 4\pi R^2 k_H r_e \text{ Watts.} \qquad (3.35)$$

The condition that $B^2/8\pi = n_e T_e$ allows the electron gyroradius to be rewritten in terms of the density:

$$r_e = 2.38 \frac{\sqrt{T_{e\,edge}}}{B} \text{ cm} = 3.75 \cdot 10^5 \frac{1}{\sqrt{n_{edge\,e}}} \text{ cm.} \qquad (3.36)$$

With the aid of the relations $(n_{edge\,e}/n_{ce}) = (r_c/r_e)^2$ and $T_{e\,edge} \equiv \frac{2}{3} E_{well}$, the ratio of the total synchrotron power to the total bremsstrahlung power may be estimated:

$$\frac{P_{syn}}{P_{br}} \sim 0.19 f k_H \left(\frac{r_c}{r_e}\right)\left(\frac{R}{r_e}\right)^2 \sqrt{\frac{E_{well}}{T_{eo}}} \frac{E_{well}^{3/2}}{r_c \sqrt{n_{ce}}} . \qquad (3.37)$$

(For this estimate the relativistic corrections to the synchrotron and bremsstrahlung losses were neglected, since they were of the same order of magnitude.)

Even at the rather extreme parameters of $E_{well} = 10^6$ eV, $r_c = 2$ cm, $n_{ce} = 5 \cdot 10^{17}$ cm^{-3}, $E_{well}/T_{eo} \approx 7$, $R/r_e = 2$, and $r_c/r_e = 1/50$, the ratio is only:

$$\frac{P_{syn}}{P_{br}} \sim 0.03 f k_H . \qquad (3.38)$$

Since $f \leq 1$ and k_H should at most be 4 or 5, it is clear that bremstrahlung, not synchrotron radiation, will be the dominant radiation loss mechanism. (Note that there

is the luxury of further reducing the synchrotron losses by reflecting and reabsorbing most of the radiation in the plasma, thus making f much smaller than 1.)

This analysis of the synchrotron radiation losses has assumed that the plasma diamagnetically excludes the magnetic field except in a very thin sheath at the plasma surface. Even if such diamagnetic effects do not occur, the synchrotron losses will be limited by the fact that the vacuum magnetic field of the cusp system varies as $(r/R)^n$, where $n \geq 3$ [10]. Thus a strong magnetic field will still exist only near the plasma surface, although it might penetrate far enough so that the sychrotron losses become comparable to the bremsstrahlung losses. (In that event, however, electron cusp losses would become so severe that they would be a much more pressing concern than synchrotron losses.)

Chapter 4

Performance for Various Fuels

The following tables present parameters and results for IEC reactors using various fuels. The reactors are assumed to use a magnetic cusp confinement system but not to utilize the ICC effect to enhance the core densities beyond those of normal convergence-limited flow. In each case the parameters have been chosen so that the reactor performance is approximately optimized.

The ions are assumed to have an initially monoenergetic distribution at an energy $E_{io} = E_{well}/2$. (Of course to produce such an initial distribution one would have to surmount the difficulties of very accurately injecting ions that deeply into the well, but for the present calculations those technical problems are neglected.) The ions will begin to evolve toward a Maxwellian distribution with $T_{io} = (2/3)E_{io}$ on a timescale of τ_{ii}. As is indicated for each fuel species in the tables, the thermalization of a test ion typically occurs two to three orders of magnitude more rapidly than the fusion of that test ion. Thus the ion distributions in the center of the device will be essentially Maxwellian, except that the high-energy tail will be truncated at the well depth.

Neglecting this truncation, the appropriate reactivity to use in these calculations is the beam-Maxwellian quantity. However, under these conditions where the beam energy is 3/2

of the Maxwellian temperature, the reactivity can be well approximated to within a few percent by the Maxwellian-averaged reactivity; hence the Maxwellian-averaged $< \sigma v >$ values are used for simplicity. Cross section data is drawn from references [28], [29], and [30].

Parameter	D-T	D-^{3}He	D-D
E_{well}	60 keV	210 keV	300 keV
T_{io}	20 keV	70 keV	100 keV
T_{eo}	18 keV	56 keV	76 keV
n_{ce}	$5 \cdot 10^{17}$ cm^{-3}	$5 \cdot 10^{17}$ cm^{-3}	$1 \cdot 10^{18}$ cm^{-3}
B	2.2 T	4.1 T	7.0 T
Fuel mixture	1:1	1:1	–
r_c	1.5 cm	2.5 cm	2.5 cm
$(\ln \Lambda)_{average}$	16	16	16
$< \sigma v >_{fus}$ (10^{-16} cm^3/s)	4.24	1.02	0.45
Q	17.6 MeV	18.3 MeV	3.7 MeV
N_{cusps}	8	8	8
k_H	2	2	2
P_{fus}	4.2 GW(t)	2.2 GW(t)	3.5 GW(t)
$P_{neutrons}/P_{fus}$	0.80	0.01	0.36
P_{brem}/P_{fus}	0.008	0.24	0.52
$P_{e\ loss\ cusp}/P_{fus}$ (from Eq. A.5)	0.11	1.32	1.42
$P_{e\ loss\ cusp}/P_{fus}$ (from Eq. 3.17)	0.47	5.76	6.39
$\tau_{i\ loss}/\tau_{fus}$	D: $5 \cdot 10^{-3}$ T: $4 \cdot 10^{-3}$	D: $3 \cdot 10^{-3}$ ^{3}He: $3 \cdot 10^{-2}$	$9 \cdot 10^{-3}$
τ_{ii}/τ_{fus}	D: $1 \cdot 10^{-3}$ T: $2 \cdot 10^{-3}$	D: $2 \cdot 10^{-3}$ ^{3}He: $2 \cdot 10^{-4}$	$2 \cdot 10^{-3}$
$\tau_{ee}/\tau_{e\ loss\ cusp}$	$1 \cdot 10^{-5}$	$3 \cdot 10^{-5}$	$1 \cdot 10^{-5}$

Table 4-1: IEC Reactors Utilizing Deuteron-Based Fuels

Parameter	p-^{11}B	p-^{6}Li
E_{well}	900 keV	1.5 MeV
T_{io}	300 keV	500 keV
T_{eo}	138 keV	206 keV
n_{ce}	$5 \cdot 10^{17}$ cm^{-3}	$1 \cdot 10^{18}$ cm^{-3}
B	8.5 T	15.5 T
Fuel mixture	5:1 p:^{11}B	3:1 p:^{6}Li
r_c	3 cm	3 cm
$(\ln \Lambda)_{average}$	16	16
$<\sigma v>_{fus}$ (10^{-16} cm^3/s)	2.39	1.1
Q	8.7 MeV	4.0 MeV
N_{cusps}	8	8
k_H	2	2
P_{fus}	1.9 GW(t)	2.7 GW(t)
$P_{neutrons}/P_{fus}$	$< 10^{-3}$	–
P_{brem}/P_{fus}	1.73	5.36
$P_{e\ loss\ cusp}/P_{fus}$ (from Eq. A.5)	10.6	15.1
$P_{e\ loss\ cusp}/P_{fus}$ (from Eq. 3.17)	61.1	92.5
$\tau_{i\ loss}/\tau_{fus}$	p: $2 \cdot 10^{-2}$ ^{11}B: 6	p: $4 \cdot 10^{-2}$ ^{6}Li: 2
τ_{ii}/τ_{fus}	p: $7 \cdot 10^{-3}$ ^{11}B: $9 \cdot 10^{-4}$	p: $1 \cdot 10^{-2}$ ^{6}Li: $3 \cdot 10^{-3}$
$\tau_{ee}/\tau_{e\ loss\ cusp}$	$1 \cdot 10^{-4}$	$5 \cdot 10^{-5}$

Table 4-2: IEC Reactors Utilizing Proton-Based Fuels

The tables also compare the time required for ions to be lost via upscattering into the high-energy tail with the time required for them to fuse. Since $E_{io} = E_{well}/2$, $Z = 1$ ions will be lost when $\Delta E_t/E_o = 1$. With the exception of ions such as ^{11}B and ^{6}Li which see a well much deeper than twice their initial energy, the ions will escape from the system far more rapidly than they will fuse. Typically between 30 and 300 ions will escape for every ion that fuses. As has already been noted, even if charge exchange can solve the problem of ion losses, it will create the difficulty of the loss of fast neutrals and compound the problem of rapid ion thermalization.

Because both of the ion species are nearly Maxwellian with equal temperatures, the averaged fusion cross sections will be considerably smaller than they would be if the ions could be kept monoenergetic at the resonance peak energy. In fact, since the high-energy ion tail escapes from the system, the average reactivities of fuels in an IEC device will be somewhat less than those in a fusion reactor which can confine the hot ion tail of the Maxwellian. For simplicity, Maxwellian-averaged reactivies were used in calculating the fusion power, but it must be remembered that the true reactivity will be smaller and so the power loss fractions will be somewhat larger than shown.

While the bremsstrahlung power loss is quite small for D-T and more or less tolerable for both D-D and D-^{3}He, it is found to be prohibitive for the other fuels, since the high ion energies in the center of the device lead to high electron temperatures there as well. Because of the truncated Maxwellian ion distributions, the bremsstrahlung/fusion ratios will be roughly equal to or perhaps even worse than those of other reactors burning these fuels.

The strength of the cusp magnetic field is calculated assuming that $\beta = 1$ at the outer plasma surface [26, 27], or $B^2 = 8\pi n_{edge\ e} E_{well}$ with E_{well} in ergs. As given in Equation 3.1, $n_{edge\ e} = n_{ce}(r_c/r_e)^2$. For the purposes of these calculations, it has been assumed that $r_e = 50 r_c$.

There are two different ways to calculate the electron power losses. Equation 3.17 gives more pessimistic results than Equation A.5, but the latter equation is based on many assumptions about the potential well and density profiles, whereas the former is not. The tables give the ratio of electron loss power to fusion power as determined by each method; in using Equation A.5, it was assumed that $A = 1.5$ and $R = 2r_e$.

Even by using the more optimistic answer and adding direct converters with 50-60% efficiency, the electron losses appear to be intolerably large for fuels other than D-T. It should also be noted that this calculation was based on the optimistic assumptions that k_H could be kept as small as 2, the effective cusp number would not be larger than 8, very high core densities could be achieved, and Ohmic power losses in the field coils could

44

be neglected. Under actual conditions, the losses will probably be even more severe than those calculated here.

(It would be possible to reduce the electron cusp losses if the outer layer of the diamagnetic plasma could be maintained in equilibrium with $\beta < 1$, so that higher magnetic field strengths could be used. However, the behavior of the outer sheath of the diamagnetic plasma is poorly understood, and the plasma might simply adjust itself to keep $\beta = 1$, as assumed in [26]. In any event, the magnetic field strengths indicated in the tables are already quite large, so it would be rather difficult to increase them much more.)

Chapter 5

Conclusions

The suitability of various implementations of inertial-electrostatic confinement (IEC) systems for use as D-T, D-D, D-^{3}He, p-^{11}B, and p-^{6}Li reactors has been examined. It has been shown that while an IEC reactor would have the advantages of high power densities and relatively simple engineering design when compared with other fusion schemes, it suffers from several flaws. These problems are ion thermalization and upscattering, bremsstrahlung, and electron cusp losses.

5.1 Ion Thermalization and Upscattering

The problem of ion thermalization and upscattering can be described in a straightforward manner. A test ion is injected into the well at the desired energy and begins to oscillate through the dense core, out toward the plasma edge, and back again. Collisions with other ions, all presumably starting at the same energy, will cause the test ion to diffuse in velocity space. The perpendicular velocity-space diffusion is less important than parallel diffusion, since most scattering occurs near the device center, and the well then returns the scattered particles to the center for another try. (There will be some core spreading

due to collisions away from the exact center, but the calculations in [10] show that the spreading is tolerably small.) For this reason, the present analysis has focused on parallel velocity-space diffusion, or energy up- and downscattering.

Since the test ion only spends a fraction of its time in the core, it would be incorrect to compute the ion-ion collision time using the core density; rather, one must use some sort of average density seen by the ion as it transits the entire system. Because the average density is typically much smaller than the core density, the thermalization and upscattering times will be significantly lengthened.

Next the characteristic thermalization and upscattering times for the test ion must be compared with the characteristic fusion time for that ion, in order to determine whether the ion is likely to fuse first or be upscattered out of the well first. Since the test ion spends only a small fraction of its time in the core, its fusion time should be lengthened by the same factor and for the same reasons as the collision time. When one takes the ratio of the fusion and thermalization times, which are both inversely proportional to density, the two factors cancel each other. One finds the ratio to be the same as in other fusion reactor designs, namely that an ion thermalizes about two to three orders of magnitude faster than it fuses. Therefore, it appears that the ion velocity distribution in the broad flat bottom of the well will look essentially like a Maxwellian truncated at the well depth rather than the desired monoenergetic distribution.

If the initial ion energy is not much smaller than the potential well depth, say half of the well depth, then ions will not have to be scattered terribly far out into the tail to be lost. They can cover this comparatively small distance in velocity space in just a few ion-ion collision times. Thus not only will the ions thermalize far more rapidly than they will fuse, but they will also escape the well much more rapidly than they fuse (except for ions like ^{11}B which see a much deeper well).

Furthermore, energy is transferred between the two ion species on a time scale roughly comparable to the thermalization time of each individual species, so that it would not appear possible to maintain the two ion species at significantly different energies or tem-

peratures in order to take better advantage of the resonance peaks in the reaction cross sections. It was shown that even if the ion species could be kept at vastly different energies, the heat transfer between them would drain energy from the more energetic species at a rate comparable to the total fusion power. This heat transfer rate would necessitate the introduction of some method for returning this large amount of power from the lower-energy ion species back to the higher-energy species and somehow pumping the newly generated entropy out of the system; in practice it would be nearly impossible to fulfill this requirement.

5.2   Bremsstrahlung

The radiated bremsstrahlung power will of course depend on the rate of the energy transfer between ions and electrons which occurs primarily near the dense core. Just as the ion-ion collision time is much shorter than the fusion time, it can also be easily shown that the electron-electron collision time is many orders of magnitude shorter than the electron loss time in the magnetic cusp confinement system. Therefore both the ions and electrons will have roughly Maxwellian distributions in the device center; the temperature of the electrons relative to that of the ions must then be determined.

For a given ion temperature, the equilibrium value of the electron temperature is obtained by equating the standard Spitzer-type ion-electron heat transfer rate with the bremsstrahlung cooling rate of the electrons; this derivation yields electron temperatures which are typically at least half of the ion temperature. As a result, at the very high ion energies necessary for p-^{11}B and p-^{6}Li reactions, the bremsstrahlung is prohibitively large, just as it is in more conventional reactor designs.

One possible solution to the bremsstrahlung problem for advanced fuels is that the ion-electron heat transfer rate for highly non-Maxwellian species or species at widely differing energies might be significantly lower than the standard Spitzer heat transfer rate. However, this solution would require methods of maintaining nonthermal particle

distributions, a feat which IEC does not presently appear able to accomplish.

5.3 Electron Cusp Losses

In the analysis of the power loss due to electrons leaking through the point cusps, many optimistic assumptions were made. It was assumed in the calculations that strong plasma diamagnetism restricts the magnetic field to a thin outer sheath of the plasma and only allows electrons to leak through cusp holes which have radii of a few electron gyroradii. Furthermore, the loss hole radius was chosen to be only twice the electron gyroradius (according to work by Grad [24] and Grossman [25] it could be as large as five). Another assumption was that there were only eight point cusps, even though the effective number of cusps may be significantly larger due to practical limitations on the magnetic field geometry, or it may be necessary to increase the number of cusps to keep the system more nearly isotropic. Using these assumptions an expression for the electron power loss was derived, and it was found to be roughly proportional to $E_{well}^{5/2}$, where E_{well} is the well depth. With the appropriate choice of parameters, and provided that the above-stated optimistic assumptions hold, the cusp power losses for D-T are tolerable, because a well depth of only a few tens of keV is required. However, the significantly greater well depths required for all other fuels cause their electron power losses to be prohibitively large.

Future IEC research should more closely examine the diamagnetic "whiffle ball" and sheath effects in magnetic cusp confinement systems, as these phenomena are poorly understood at the present time. If the outer plasma sheath can be kept at $\beta < 1$, the electron confinement could be somewhat better than predicted here. On the other hand, if the loss hole radius cannot be made as small as a couple of electron gyroradii, the electron confinement will be much worse than was calculated.

If electrostatic grids are used instead of magnetic cusps, the electron losses should be orders of magnitude worse, large numbers of ions would also be lost by collisions with the grids, and the severe problem of grid heating would also arise. While grids are convenient

for small-scale experiments, they do not appear to be desirable in actual IEC reactors.

5.4   Acoustic-Wave Compression of the Core

Although the use of acoustic standing waves to increase the core density and/or alter the density profile has been proposed in both [11] and [12], it appears that such a phenomenon could do little to improve the fundamental problems noted above (and it may even have a detrimental impact). For example, the ratios of ion thermalization and upscattering times to the fusion time are independent of both the core density and the spatial profile of the density in the reactor, and so they would remain unaffected by the so-called ICC effect. Likewise the ratio of bremsstrahlung power to fusion power would also remain the same.

As noted previously, one might think that using the ICC effect to increase the core density relative to the edge density would improve the ratio of cusp losses to fusion power, since the cusp losses occur at the edge and fusion occurs in or near the core. Yet as it was shown, the constraint that $\beta = 1$ at the outer plasma boundary removed the dependence of the power loss fraction on the edge density, and thus on the density profile.

The only critical parameter is the core density, which may be created via the ICC effect or simply by unaided ion flow convergence at the center of the device. Obviously the primary effect of altering the core density will be to change the fusion power density and total fusion power.

Even if it were quite desirable to employ the ICC effect, it is far from certain that the acoustic waves will work as expected to compress the core. If the ICC effect does indeed occur, it is highly questionable whether it can achieve the necessary many-fold compression without simultaneously degrading the central ion convergence and defeating the purpose of its use.

5.5 Other Potential Problems

There are several other issues which were not examined in this paper but which would need to be carefully considered in future IEC work. These areas include determining the limitations on maximum core density and more closely scrutinizing the rate of core spreading due to angular momentum buildup. One would also have to perform analyses of counterstreaming and Weibel instabilities, taking into account the fundamental nonlinear, nonlocal nature of the problem. Another question is whether part or all of the potential well will eventually fill in due to background neutrals and other effects. In addition to these physics issues, there are serious technological problems which must be explored, such as finding suitable techniques for accurately fueling deep inside the well and designing direct converters appropriate for the spherical geometry of IEC devices.

In conclusion, it is hoped that discussion of these apparent problems will in the future lead to the discovery of methods which can circumvent them, allowing IEC devices to maintain energetic non-Maxwellian ion populations with relatively cold electrons and to offer a good power balance even for advanced fuels.

Appendix A

Alternate Derivation of Cusp Losses

An alternate way to derive the power loss due to electrons leaking through the magnetic cusps is to make use of η_{loss}, the characteristic loss time of the electrons, as given in Equation 3.21. If the total electron population in the machine is N_e and the energy per lost electron is E_{well} (in ergs), then the power loss due to escaping electrons is

$$P_{e\ loss\ cusp} = \frac{N_e E_{well}}{\eta_{loss}} \ . \tag{A.1}$$

Using the density profile of Equation 3.1, the total electron population is found to be

$$N_e = \frac{4}{3}\pi n_{ce} r_c^2 r_e \left[2\left(1 - \frac{r_c}{r_e}\right) + \left(\frac{R}{r_e}\right)^3 \right] \ . \tag{A.2}$$

For typical length ratios within the machine, $r_c/r_e \ll 1$, so it may be neglected compared with the other two terms within the brackets.

Putting the above equations together and expressing E_{well} in eV, one obtains

$$P_{e\ loss\ cusp} = 3.98 \cdot 10^{-11} A \left(\frac{r_e}{R}\right) \left(\frac{r_c}{R}\right)^2 \left[2 + \left(\frac{R}{r_e}\right)^3\right] N k_H^2 \frac{E_{well}^2 \sqrt{T_{eo}} n_{ce}}{B^2} \text{ Watts.} \quad \text{(A.3)}$$

Setting $\beta = 1$ at the plasma edge so that $B^2 = 8\pi n_{edge\ e} E_{well}$, and using $n_{edge\ e} = n_{ce}(r_c/r_e)^2$, the cusp power loss becomes

$$P_{e\ loss\ cusp} = 0.988 A \left[1 + 2 \left(\frac{r_e}{R}\right)^3\right] N k_H^2 E_{well} \sqrt{T_{eo}} \text{ Watts.} \quad \text{(A.4)}$$

The ratio of the electron loss power to the fusion power of an IEC device with convergence-limited core densities is

$$\frac{P_{e\ loss\ cusp}}{P_{fus}} = 3.69 \cdot 10^{17} A \left[1 + 2 \left(\frac{r_e}{R}\right)^3\right] \frac{(x + Z_2)^2}{x} \frac{N k_H^2 E_{well} \sqrt{T_{eo}}}{<\sigma v> Q n_{ce}^2 r_c^3} . \quad \text{(A.5)}$$

Several factors in this expression are determined by the shape and depth of the electrostatic well. Using typical values of $A \approx 1.5$, $r_e/R \approx 0.5$, and $T_{eo} \approx E_{well}/3$, Equation A.5 reduces to

$$\frac{P_{e\ loss\ cusp}}{P_{fus}} \approx 4 \cdot 10^{17} \frac{(x + Z_2)^2}{x} \frac{N k_H^2 E_{well}^{3/2}}{<\sigma v> Q n_{ce}^2 r_c^3} . \quad \text{(A.6)}$$

This answer is about 4 times smaller than the result of the electron loss derivation that was presented earlier. However, it is dependent on the exact potential well profile, density profile, and relative temperatures of the different particle species, whereas the earlier result was not. In any event, there is enough uncertaintly in k_H, which enters both equations as a square, that a factor of 4 is comparatively unimportant. Whichever derivation one uses, the electron losses are sizable for D-T and intolerable for D-^{3}He and p-^{11}B, even when one optimistically assumes some relatively small value for k_H.

53

Bibliography

[1] R.W. Bussard, Some Physics Considerations of Magnetic Inertial-Electrostatic Confinement: A New Concept for Spherical Converging-Flow Fusion. *Fusion Technology*, 19:273-293, March 1991.

[2] W.C. Elmore, J.L. Tuck, and K.M. Watson, On the Inertial-Electrostatic Confinement of a Plasma. *Physics of Fluids*, 2:239-246, May-June 1959.

[3] P.T. Farnsworth, Electric Discharge Device for Producing Interactions Between Nuclei. U.S. Patent No. 3,258,402, June 28, 1966.

[4] P.T. Farnsworth, Method and Apparatus for Producing Nuclear-Fusion Reactions. U.S. Patent No. 3,386,883, June 4, 1968.

[5] R.L. Hirsch, Inertial-Electrostatic Confinement of Ionized Fusion Gases. *Journal of Applied Physics*, 38:4522-4534, October 1967.

[6] R.L. Hirsch, Experimental Studies of a Deep, Negative, Electrostatic Potential Well in Spherical Geometry. *Physics of Fluids*, 11:2486-2490, November 1968.

[7] D.C. Barnes, R.A. Nebel, and L. Turner, Production and Application of Dense Penning Trap Plasmas. LA-UR 93-314, 1993.

[8] R.W. Bussard, Method and Apparatus for Controlling Charged Particles. U.S. Patent No. 4,826,646, May 2, 1989.

[9] N.A. Krall, The Polywell: A Spherically Convergent Ion Focus Concept. *Fusion Technology*, 22:42-49, August 1992.

[10] M. Rosenberg and N.A. Krall, The Effect of Collisions in Maintaining a Non-Maxwellian Plasma Distribution in a Spherically Convergent Ion Focus. *Physics of Fluids B*, 4:1788-1794, July 1992.

[11] R.W. Bussard, Method and Apparatus for Creating and Controlling Nuclear Fusion Reactions. U.S. Patent No. 5,160,695, November 3, 1992.

[12] D.C. Barnes and L. Turner, Non-Neutral Plasma Compression to Ultrahigh Density. *Physics of Fluids B*, 43890-3901, December 1992.

[13] L.M. Lidsky, The Trouble with Fusion. *Technology Review*, **86**:7:32-44, October 1983.

[14] S. Glasstone and R. Lovberg, *Controlled Thermonuclear Reactions*. Van Nostrand Reinhold Co, New York, 1960.

[15] D. L. Book, *NRL Plasma Formulary*. Revised 1987, Naval Research Laboratory, Washington.

[16] K. Miyamoto, *Plasma Physics for Nuclear Fusion*, MIT Press, Cambridge, MA, 1989.

[17] M. Rosenberg and N.A. Krall, Ion Loss by Collisional Upscattering. Krall Associates Report KA-90-39, January 1991.

[18] D.V. Sivukhin, in *Reviews of Plasma Physics*, Vol. 4 (ed. by M.A. Leontovich), Consultants Bureau, New York, 1966.

[19] W.M. MacDonald, M.N. Rosenbluth, and W. Chuck, Relaxation of a System of Particles with Coulomb Interactions. *Physical Review*, **107**:350-353, July 15, 1957.

[20] S. Maxon, Bremsstrahlung Rate and Spectra from a Hot Gas (Z=1). *Physical Review A*, **5**:4:1630-1633, April 1972.

[21] J.R. McNally, Jr., Physics of Fusion Fuel Cycles. *Nuclear Technology/Fusion*, **2**:9-28, January 1982.

[22] J.M. Dawson, Series Lecture on Advanced Fusion Reactors. Research Report IPPJ-623, Institute of Plasma Phsyics, Nagoya University, Japan, January 1983.

[23] M.N. Rosenbluth, Energy Exchange Between Electrons and Ions. *Bulletin of the American Physical Society*, **21**:1:1114-1115, January 1976.

[24] H. Grad, Containment in Cusped Plasma Systems. in *Plasma Physics and Thermonuclear Research Vol. 2*, C.L. Longmire, J.L. Tuck, and W.B. Thompson, eds. The Macmillan Company, New York, 1963.

[25] W. Grossmann Jr., Particle Loss in a Three-Dimensional Cusp. *Physics of Fluids*, **9**:2478-2485, December 1966.

[26] O.A. Lavrent'ev Electrostatic and Electromagnetic High-Temperature Plasma Traps. *Annals of the New York Academy of Sciences*, **251**:152-178, May 8, 1975.

[27] N.A. Krall, private communication, June 7, 1993.

[28] G.H. Miley, H. Towner, and N. Ivich, *Fusion Cross Sections and Reactivities*. University of Illinois, Champaign-Urbana, 1974.

[29] R. Feldbacher, The AEP Barnbook DATLIB, INDC(AUS)-12/G. IAEA International Nuclear Data Committee, Vienna, October 1987.

[30] J.R. McNally, Jr., K.E. Rothe, and R.D. Snarp, *Fusion Reactivity Graphs and Tables for Charged Particle Reactions.* Oak Ridge National Laboratory, Report ORNL/TM-6914, 1979.